



Characterization of Particle Shape and Surface Properties of Powders from Volcanic Scoria

A. Bouyahyaoui¹, T. Cherradi¹, M. L. Abidi¹, W. H. Juimo Tchamdjou^{1,2*}

¹Mohammadia School of Engineers, Mohammed V University of Rabat, Po. Box. 765, Rabat, Morocco

²National Advanced School of Engineering of Maroua, University of Maroua, Po. Box. 46, Maroua, Cameroon

Received 28 Sep 2017,
Revised 18 Mar 2018,
Accepted 01 Apr 2018

Keywords

- ✓ Volcanic scoria,
- ✓ Powder,
- ✓ Particle size distribution,
- ✓ Laser diffraction,
- ✓ Image analysis.

hermannjuimo@gmail.com;
Phone: +212632967544;
Fax: +212537778853

Abstract

To develop high-performance and versatile cement-based materials like self-compacting concrete SCC and reactive powder concrete RPC, the research on inert and semi-inert powders from natural resources has been increased. In this study, the particle shape and surface morphology of powders from volcanic scoria VS (Black, Dark-Red, Red and Yellow) collected in Cameroon has been analysed. Four powders were prepared by grinding with the same energy for all. Particle size distribution PSD were performed by using laser diffraction LD. Blaine fineness BF of powders were performed. Shape, surface morphology parameters and image analysis IA of these fine materials were performed. Shape characteristics of these powders were presented and were correlated with Blaine fineness. In addition to PSD, granulo-morphology has been providing a better understanding of particle shape and surface morphology parameters and their influence on blended cement.

1. Introduction

The particle size distribution (PSD), surface area and shape are fundamental characteristics of supplementary cementitious materials (SCMs). The main SCMs that are used today are industrial by-products. In most cases the quality of these materials cannot be controlled during their production, resulting in materials with varied characteristics. The adequate physical characterization of SCMs is important to better predict their performance and optimize their use in concrete production. There are standardized methods used to determine the particle characteristics for Portland cements that are usually adopted to characterize SCMs; however, these methods may not be as accurate when applied to SCMs [1].

The use of SCMs in the production of concrete has increased worldwide over the past few decades [2, 3]. These materials can enhance the mechanical and durability properties of concrete and contribute to mitigation of the environmental impact associated with the construction industry. SCMs are used as a partial replacement for Portland cement in concrete, reducing the fraction of Portland cement required to produce concrete with desired performance. The performance of SCMs in concrete is strongly dependent on their physical and chemical characteristics, which vary depending on the nature and source of the SCM. In general, the fineness is one of the most important physical properties controlling the reactivity of SCMs and the subsequent strength development of blended binders [4].

Reducing the average particle size increases the rate of dissolution of the SCM, raising the pozzolanic activity and thus the development of more strength-giving hydration products that enhance the long-term performance of the concrete. Small particles can also facilitate nucleation and growth of cement hydration products on the SCM surfaces, speeding up the early cement hydration and therefore the strength development. However, reducing the particle size of SCMs beyond an optimal value, usually leads to an increased water demand of the concrete mixtures to achieve a desired workability, which can negatively affect both strength and its durability [5]. Further, if the particle size is decreased by grinding, this requires additional energy costs.

For most industrial control purposes, the primary characteristics measured in powders are specific surface area, particle size distribution, particle shape, and density. The specific surface area (defined on a mass basis) is the

most common property used to describe the fineness of Portland cement [6]. This surface area is an integral parameter and gives no information about the details of the actual particle size distribution, which is probably of greater importance in defining concrete performance. The description of particle shape encompasses information about the sphericity and angularity, which affect the workability and also the physical phenomena utilized for particle size measurement [7]. Density can refer either to the unit volume of a packed powder, or to the specific gravity of the solid material itself. Both are key parameters in designing concrete, and particularly an accurate measurement of density is required for the conversion between volume and mass for calculation of the particle size distribution, and of the unit weight of concrete.

In this paper, in addition to PSD, the particle shape and morphology of four natural pozzolans from volcanic scoria (ground at the same energy) were analysed by using laser diffraction (LD) on a Mastersizer 2000E and image analysis (IA) on a granulomorphometer (Occhio 500 nano).

2. Characterization of powders

The techniques that are currently used for the characterization of SCMs include sieving, air permeability testing (Blaine), LD, and IA. Compared with the size, shape of a particle is a complex feature to identify and characterize. IA method was developed to performed shape of particles. From 2D projections, IA can provide more accurate and elaborate shape information of particles.

2.1. Description of volcanic scoria used

Four samples volcanic scoria's according the colour of scoria (Black, Dark-red, Red and Yellow) have been collected in 'Djoungo' quarry (Cameroon). The different scoria colour and powder obtained from each sample by production process (crushing and milling) are presented in Figure 1. Each powder has been described by a two-component code designation: the letter reflecting powder colour as black (B), dark-red (DR), Red (R) and yellow (Y) followed by the NP reflecting natural pozzolan [8].



Figure 1: Macroscopic view of different rocks used and powders obtained.

2.2. Production process

Powders were prepared by grinding. Volcanic scoria aggregates (VSA) used were between 20 to 50mm particle size after sieving to remove fine VSA in each collected sample after drying in oven at 105°C during 24 hours. The grinding was performed in a disk mill of VSA size smaller than 10 mm after reducing of a large VSA by jaw crusher (Figure 2). The mill process was performed during 20 minutes. Milling sample has been introduced at the same weight for each production. The rotation speed of the mill was about 70 rpm. Depending volcanic scoria colour, four VS powder samples were obtained.

2.3. Chemical and mineralogy properties of powders

Mineralogy characterisation of each powder was performed by X-Ray diffraction (XRD). Fig.3 shows XRD results of powders. Mineralogy mean phases are of each powder are: Hematite (Fe_2O_3), Quartz (SiO_2), Diopside ($\text{MgCaSi}_2\text{O}_6$), Albite ($\text{Na(AlSi}_3\text{O}_8)$) and Olivine (Ca_2SiO_4).

X-Ray fluorescence (XRF) was performed only on one powder (RNP) to have and ideas on the chemical composition of powder. Table 1 present a chemical composition of RNP powder [8].



Figure 2: (a) Jaw crusher used and (b) Disk mill used to produce powders.

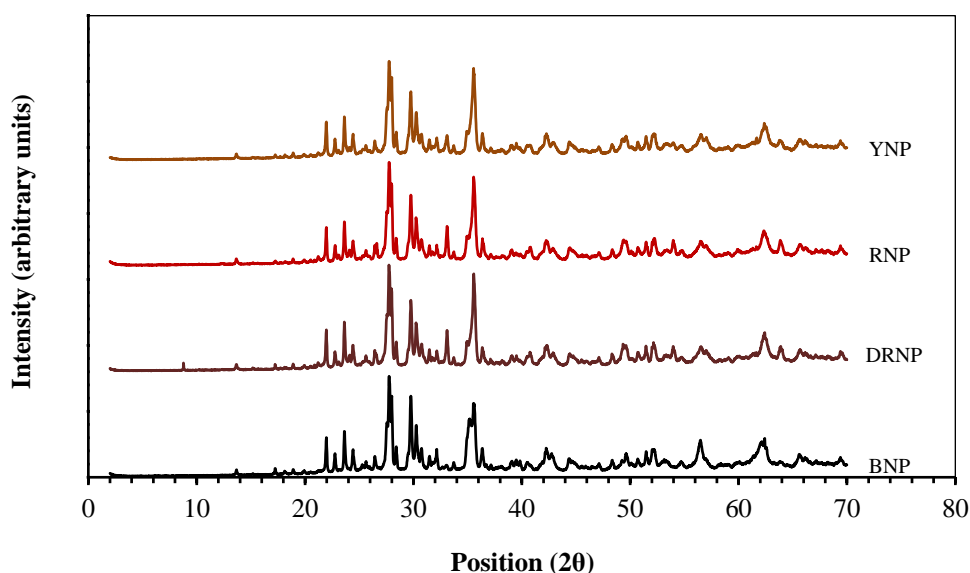


Figure 3: XRD of powders.

Table 1: Chemical composition of RNP powder.

Oxide (%)	SiO ₂	Al ₂ O ₃	Fe ₂ O ₃	CaO	MgO	MnO	Na ₂ O	K ₂ O	SO ₃	TiO ₂	P ₂ O ₅	L.O.I.
RNP	46.92	15.36	13.20	8.87	6.93	0.18	3.49	1.42	-	2.82	0.59	0.46

2.4. Density and specific surface area (SSA)

Density, PSD, shape and size are the fundamental physical characteristics of powders [1]. Density measurements of powders are generally conducted on the basis of volumetric displacement of a fluid [9]. In this study, the density of VS powders was performed on a Helium gas pycnometer. The average absolute density of each VS powder was approximate 3.0g/cm³. Table 2 shows the density of each powder obtained by Helium gas pycnometer. SSA was measured by Blaine air permeability apparatus [8]. The Blaine air permeability tester is used for the measurement of the SSA of particles at the base of the air permeability method: the time *t* necessary for a volume of air to flow through a packed bed of particles is recorded [10]. The European Standard EN 196-6 [9] gives the evaluation of SSA with Kozeny-Carman equation. SSAs measured with the Blaine air permeability apparatus are ranging between 3550 to 5250 cm²/g. Table 2 shows all the parameters using and obtained. PSD by LD also shows the values of SSA, but these values are very higher than those obtained by Blaine air permeability (Table 2).

2.5. PSD, shape and surface texture of powders.

The particle size distribution (PSD) of the powdered materials was performed by LD on a Mastersizer 2000E (Malvern, UK; 633 nm red laser) and by IA on a Granulomorphometer (Occhio 500 nano). The mean particle diameter (*D*_{med}) and median particle diameter (*D*₅₀) were measured to evaluate the efficiency of the milling process. The main PSD characteristics of VS powders are listed in Table 2. The characteristic percentile diameters *D*₁₀, *D*₅₀ and *D*₉₀ are also reported. VS powders are fine products with *D*₅₀ between 8.736μm (RNP) and 19.214 μm (BNP) [8].

Table 2: Density, SSA and PSD of powders.

VS powder	BNP	DRNP	RNP	YNP
Colour	Black	Dark-red	Red	Yellow
ρ_s (g/cm ³)	2.8883	3.0139	2.9201	3.0294
Blaine air permeability testing conditions and parameter values				
T(°C)	21.6	21.6	21.6	22.1
HR (%)	65.5	65.5	65.5	64.5
Weight (g)	2.68	3.35	2.90	2.94
Porosity ε	0.503	0.408	0.468	0.481
η (x10 ⁻⁶ Pa.s)	18.29	18.29	18.29	18.29
ρ_L (g/cm ³)	1.0424	1.0424	1.0424	1.0424
D_{cell} (mm)	12.68	12.68	12.68	12.68
D_{tube} (mm)	5.9	5.9	5.9	5.9
k (m.s ²)	34	34	34	34
L_{sample} (mm)	14.78	14.785	14.78	14.80
C_{air} (x10 ³ Pa)	99.85847	99.85847	99.85847	99.19186
K_{app} *	2.49	2.49	2.49	2.49
Temps t (s)	0.74	4.215	0.45	0.05
SSA, by Blaine**	3596	4482	4674	5227
Laser Diffraction, SSA and PSD				
D_{med} (µm)	48.639	22.401	37.971	27.777
D_{10} (µm)	1.568	1.179	1.235	1.243
D_{50} (µm)	19.214	8.736	12.492	11.011
D_{90} (µm)	142.577	66.054	114.723	80.998
D[3,2] (µm)	4.706	3.318	3.674	3.621
SSA by LD**	4414	5999	5593	5470
<p>*in g^{1/2}.cm^{3/2}.s-1; **in cm²/g is the porosity of the packed bed of powder, η is the viscosity of air (Pa.s), ρ_s the density of the solid (g.cm⁻³)ε, ρ_L is the density of the manometer fluid, D_{cell} and D_{tube} are the inner diameter of the cell and of the tube [cm], respectively, k is the Kozeny constant, L_{sample} is the height of the packed bed of powder [cm]. is a term which takes into account air compressibility due to pressure drop between the opposite sides of the C_{air} sample; it depends on atmospheric pressure and geometrical characteristics of the instrument. Kozeny constant is related to the shape of particles and the bed tortuosity.</p>				

An estimation of SSA area is also calculated from the PSD by LD measurement, in accordance with Equation 1.

$$S_{S,PSD} = \frac{6}{\rho_s \cdot D[3,2]}, \text{ where } : D[3,2] = \frac{\sum n_i d_i^3}{\sum n_i d_i^2} \quad (\text{Equation 1 and Equation 2})$$

The volume to surface mean diameter D[3,2] of the sample is calculated from the size distribution curve by means of Equation 2, in which n_i corresponds to the number of particles of diameter d_i .

These equations assume that the particles are spherical and that they are not porous. SSA value obtains by this method for each powder is always higher about of 4% to 25% than SSA obtain by Blaine air permeability. This can demonstrate that the porosity of VS powders by volume is around 4% to 25%. Juimo et al. [11] are reported that VSA size between 20-50 mm can present up to 51% of porosity. We can conclude that, high porosity of VSA is a high porosity scale. PSD of powders was also evaluated using IA by 2D projection. Fig.4 shows PSDs of VS powders by LD and by IA method. For all grading sizes, PDS by LD is higher than PDS by IA (Figure 4). BNP (and at a lower significance RNP) appears to be less coarse than other VS powders. Fig.5 presents the comparison of the passing ratio of 25µm, 45 µm, 50 µm, 63 µm, 75 µm and 80 µm for all powder using LS and IA method. IA presents a small passing ratio than LD.

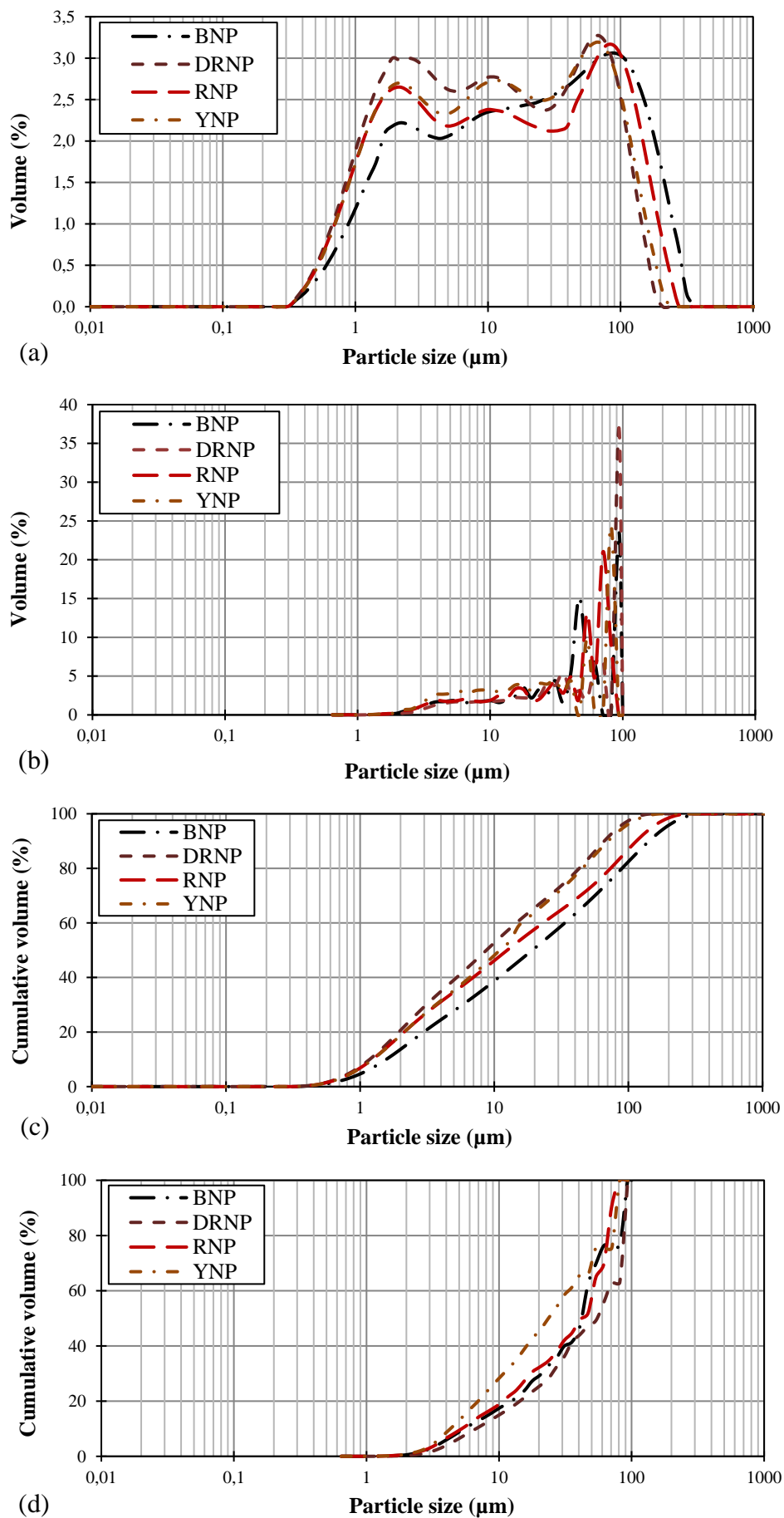


Figure 4: PSD by LD (volume (a) and cumulative volume (c)) and PSD by IA (volume (b) and cumulative volume (d)).

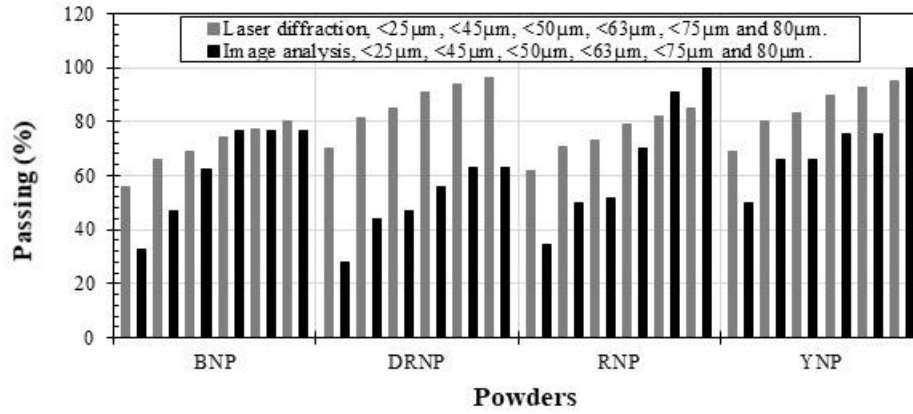


Figure 5: 25-80µm passing ratio obtained with LD and IA for each powder.

Powders samples tested by IA had respectively: 24268 particles for BNP, 32302 particles for DRNP, 22562 particles for RNP and 25041 particles for YNP. Morphology and shape of powder particles were performed by IA by 2D projection (Figure 6).

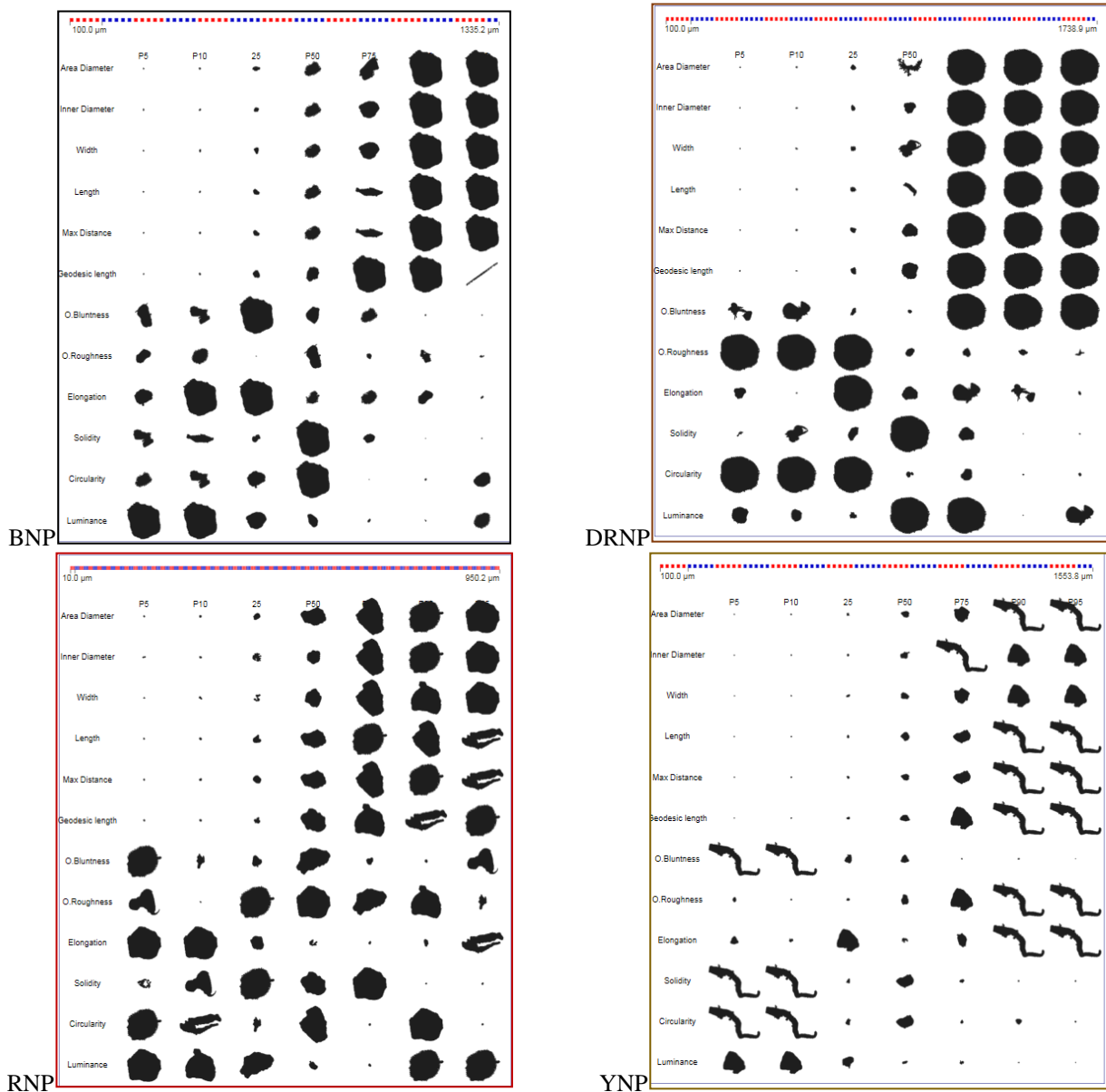


Figure 6: Morphology by 2D projections of particles by IA using Granulomorphometer (BNP, DRNP, RNP and YNP).

Some traditional shape parameters are presented. The parameters obtained by IA were: area diameter, inner diameter, width, length, max distance, geodesic length, elongation, circularity, solidity, roundness, roughness, compactness, bluntness and luminance. Some of these traditional shape parameters describe by several authors are then used for the evaluation shape and surface properties of particles. He et al. [12] are illustrated some of these parameters to characterize fine aggregate for concrete (Figure7).

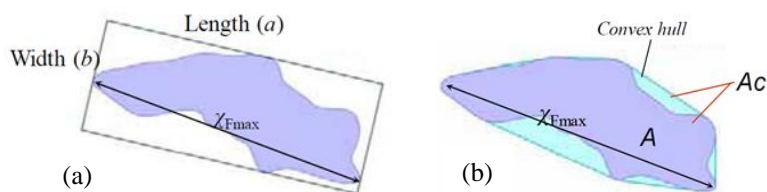


Figure 7: (a) Width, Length and Max distance (b) A convex hull bounding particle and Area A and Ac.

Table 3 shows the: Mean, D[4;3], SD, Min and Max of dimensions (area diameter, inner diameter, width, length, max distance and geodesic length) of each VS powder.

The shape parameters (Elongation, and Circularity) have been describing and data provide by IA are presented. Elongation is one of the most popular parameters used in the shape analysis. It describes the relationship between width (b) and length (a), as shown in Figure7a and in Equation 3:

$$Elongation = 1 - \frac{b}{a} \quad (\text{Equation 3})$$

For very elongated particles, the straightness is definite as the ratio between the Max distance and the FeretLength (χ_{Fmax} , shown in Figure 7b).

Circularity is defined as the ratio of equivalent circle perimeter to the perimeter of the particle, it is also defined as the degree to which the particle (or its projection area) is similar to a circle. It is shown with the Equation 4:

$$Circularity = \sqrt{\frac{4\pi A}{P^2}} \quad (\text{Equation 4})$$

Where A is the projected area of the particle. It indicates the similarity degree of a particle to a disc, considering the smoothness of the perimeter P.

Table 4. shows Mean, D[4;3], SD, Min and Max values of elongation and circularity of VS powders studying. A more elongated particle has a higher value of elongation (≤ 1). RNP has a higher mean value of elongation (0.286) than others, RNP presents a higher number of elongated particles than others and confirmed in Fig.8. BNP is a powder which has most of circular particles of these powders.

Other shape parameters, solidity, roughness, roundness and compactness are also used for the shape evaluations. Solidity is defined as the ratio of particle area A, to the area of the corresponding convex hull (perfectly to detect aggregates) bounded particle A_c (Figure7b). It measures the overall concavity of a particle (Equation 5):

$$Solidity = \frac{A}{A_c} \quad (\text{Equation 5})$$

The roundness is also a useful parameter for describing the similarity degree of a particle to a circle. Unlike circularity, roundness considers the maximum Feret Length (χ_{Fmax} , shown in Figure 7b) in the Equation 6:

$$Roundness = \frac{4A}{\pi \chi_{Fmax}^2} \quad (\text{Equation 6})$$

Compactness and roundness are related to the degree to which the particle is similar to a disc. The roundness is less robust than compactness.

The roughness is the amount ratio of material to be removed from the shape before getting a smooth surface. Table 5 shows the: Mean, D[4;3], SD, Min and Max values of solidity, roundness and roughness. YNP presents more particles with high roughness than other powders. DRNP presents more very roundness particles (Figure 6 and Table 5).

Table 3: Mean, D [4;3], Standard Deviation, Min and Max values of area diameter, inner diameter, width, length, max distance and geodesic length.

Parameter (µm)	Powder	Mean	D [4,3]	SD	Min	Max
Area Diameter	BNP	46.99	46.99	35.98	0.593	105.3
	DRNP	70.55	70.54	57.86	0.593	150.4
	RNP	39.22	39.22	24.63	0.593	72.08
	YNP	33.56	33.56	27.90	0.593	79.33
Inner Diameter	BNP	38.04	44.57	31.85	0.525	90.96
	DRNP	60.17	76.34	54.54	0.525	137.4
	RNP	30.07	34.61	21.02	0.525	63.69
	YNP	22.01	21.74	21.02	0.525	57.49
Width	BNP	45.02	49.21	36.67	0.525	105.7
	DRNP	69.06	71.73	56.84	0.525	147.3
	RNP	36.94	38.55	23.95	0.525	70.83
	YNP	30.38	30.05	24.76	0.525	72.14
Length	BNP	56.10	64.03	39.41	0.525	118.6
	DRNP	80.79	71.94	61.25	0.525	161.6
	RNP	50.09	63.03	32.32	0.525	124.2
	YNP	55.45	133.2	64.33	0.525	204.8
Max Distance	BNP	57.39	65.76	41.05	0.525	120.5
	DRNP	83.25	75.81	63.48	0.525	167.2
	RNP	51.17	64.20	33.13	0.525	124.3
	YNP	55.93	134.6	64.73	0.525	205.9
Geodesic length	BNP	63.26	138.2	49.28	0.525	197.2
	DRNP	194.6	374.9	204.00	0.525	484.2
	RNP	66.35	142.9	61.12	0.525	220.4
	YNP	72.00	242.8	97.49	0.525	300.2

Table 4: Mean, D[4;3], SD, Min and Max of elongation and circularity.

Parameter (-)	Powder	Mean	D[4,3]	SD	Min	Max
Elongation	BNP	0.227	0.416	0.141	0.000	0.957
	DRNP	0.187	0.407	0.129	0.000	0.819
	RNP	0.239	0.415	0.164	0.000	0.822
	YNP	0.286	0.409	0.201	0.000	0.813
Circularity	BNP	0.672	0.769	0.193	0.045	0.878
	DRNP	0.492	0.769	0.256	0.075	0.890
	RNP	0.619	0.768	0.220	0.132	0.877
	YNP	0.630	0.772	0.229	0.155	0.882

Table 5: Mean, D[4;3], Standard Deviation (SD), Min and Max of solidity, roundness and roughness.

Parameter (-)	Powder	Mean	D[4,3]	SD	Min	Max
Solidity	BNP	0.943	0.998	0.064	0.521	1.000
	DRNP	0.918	0.997	0.104	0.457	1.000
	RNP	0.917	0.998	0.097	0.505	1.000
	YNP	0.890	0.998	0.169	0.483	1.000
Roundness	BNP	0.664	0.517	0.509	0.000	1.000
	DRNP	0.720	0.886	0.516	0.000	1.000
	RNP	0.585	0.370	0.502	0.000	1.000
	YNP	0.369	0.053	0.506	0.000	1.000
Roughness	BNP	0.020	0.206	0.035	0.000	0.312
	DRNP	0.026	0.245	0.053	0.000	0.417
	RNP	0.025	0.180	0.038	0.000	0.294
	YNP	0.040	0.173	0.060	0.000	0.253

The luminance is the mean greyscale level of the particle.

The bluntness describes the maturity of the particle in the abrasion process (Figure 8) and presented by the Equation 7.

$$Bluntness = \frac{1}{\sqrt{\bar{v}} - 1} \quad \text{(Equation 7)}$$

In which:

$$\bar{v} = \frac{1}{N} \sum_i^N \left(1 + \frac{r_{max}}{r_i}\right)^2 \quad \text{(Equation 8)}$$

where r_i is the radius of the maximum inscribe circle at the point i and r_{max} is the maximum value of r_i . The high value of bluntness indicates a high degree of abrasion [12].

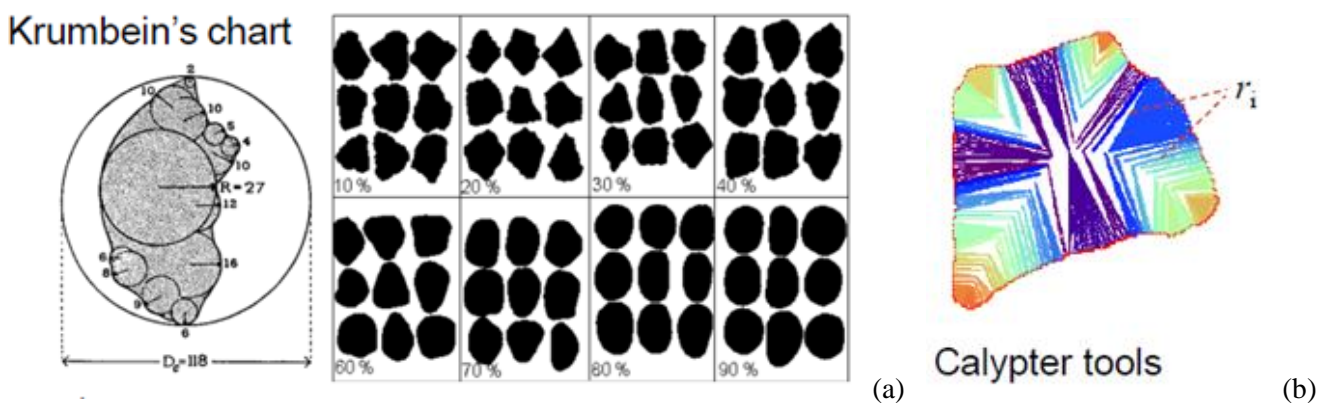


Figure 8: (a) Krumbein's chart and (b) Calypter tools.

Table 6 shows Mean, D[4;3], Standard Deviation, Min and Max values of luminance and bluntness. This result shows the roundness and bluntness of particles are very related.

DRNP presented a powdery dusty appearance with disaggregated particles than BNP and RNP. YNP presented an irregular-shaped material, with powder and pieces of low cohesion formed of small aggregated particles than others.

Table 6: Mean, D[4;3], SD, Min and Max of luminance and bluntness.

Parameter (-)	Powder	Mean	D[4,3]	Std D	Min	Max
Luminance	BNP	0.112	0.437	0.138	0.015	0.569
	DRNP	0.219	0.430	0.203	0.023	0.892
	RNP	0.133	0.438	0.138	0.017	0.911
	YNP	0.126	0.435	0.118	0.022	0.558
Bluntness	BNP	0.599	0.977	0.224	0.098	1.000
	DRNP	0.690	0.966	0.296	0.149	1.000
	RNP	0.573	0.977	0.245	0.037	1.000
	YNP	0.624	0.975	0.258	0.185	1.000

Conclusion

In this paper presents some characteristics of powders obtained from Cameroonian volcanic scoria. On the basis of the testing program and the results obtained, the following conclusions can be drawn for these powders:

- chemical and mineralogy composition of raw material could have an effect on the PSD and particle morphology of powders obtained after the milling of rock aggregate;
- the average values of SSA calculated from laser diffraction (LD) data are greater than from Blaine air permeability;
- laser diffraction (LD) and image analysis (IA) are very important to understand packing behaviour and rheology of VS powders as supplementary cementitious materials or an addition in SCC or RPC concrete;
- it appears that the specific surface area and granulometry of VS powders may be efficiently estimated from Blaine, LD and IA. This description is absolutely needed for understanding particle behaviour in contact with water, when used in cementitious materials.

Acknowledgements

The corresponding author would like to thank Sophie Leroy and Frédéric Michel, GeMME research engineers at University of Liège (Belgium) for their help in the testing program. The authors also warmly appreciated the support from the 'Académie de Recherche et d'Enseignement Supérieur (ARES)' through the Stage 'Valorisation des ressources secondaires pour une construction durable'.

References

1. E. C. Arvaniti, M. C. G. Juenger, S. A. Bernal, J. Duchesne, L. Courard, S. Leroy, J. L. Provis, A. Klemm, N. De Belie, *Mater. Struct.*, 48 (2015) 3675–3686.
2. B. Lothenbach, K. Scrivener, R. D. Hooton, *Cem. Concr. Res.*, 41(12) (2011) 1244–1256.
3. R. Snellings, G. Mertens, J. Elsen, *Rev. Mineral. Geochem.*, 74 (2012) 211–278.
4. I. B. Celik, *Powder Technol.*, 188(3) (2009) 272–276.
5. K. L. Scrivener and R. J. Kirkpatrick, *Cem. Concr. Res.*, 38(2) (2008) 128–136.
6. U. Stark and A. Mueller, *Proceedings of the 11th ICC, 11-16 May 2003, Durban, South Africa, Cement's Contribution to the Development in the 21st Century*, ISBN: 0-9584085-8-0(2003) 303–313.
7. M. Naito, O. Hayakawa, K. Nakahira, H. Mori and J. Tsubaki, *Powder Technol.*, 100(1) (1998) 52–60.
8. W. H. J. Tchamdjou, S. Grigoletto, F. Michel, L. Courard, T. Cherradi, M. L. Abidi, *Int. J. Eng. Res. Afr.*, ISSN: 1663-4144, 32 (2017) 36–52.
9. EN 196-6, Methods of testing cement - Part 6: Determination of fineness, *European Standard*, (2010).
10. F. Michel and L. Courard, *Part. Sci. Technol.*, 32 (2014) 334–340.
11. W. Juimo, T. Cherradi, L. Abidi and L. Oliveira, *Int. J. of GEOMATE*, ISSN: 2186-2982(Print), 2186-2990(Online), 11(27) (2016) 2782–2789.
12. H. He, L. Courard, E. Pirard and F. Michel, *Image Anal. Stereol.*, 35 (2016) 159–166.

(2018) ; <http://www.jmaterenvironsci.com>